Hindawi
Advances in Civil Engineering
Volume 2020, Article ID 2637651, 15 pages
https://doi.org/10.1155/2020/2637651

Research Article

Failure and Remediation of an Embankment on Rigid Column-Improved Soft Soil: Case Study

Shaofu Gu,[1,2] Weizheng Liu ,[1] and Mengyuan Ge[1]

[1]*School of Civil Engineering, Central South University, Changsha 410075, China*
[2]*JSTI Group, Guangdong Test and Certification, Guangzhou 510800, China*

Correspondence should be addressed to Weizheng Liu; liuwz2011@csu.edu.cn

Received 19 January 2020; Revised 17 May 2020; Accepted 22 May 2020; Published 20 August 2020

Academic Editor: Qiang Tang

The south extension line was constructed as a new part of the Xintai Expressway in Guangdong Province, China. The project required the construction of an embankment over soft soil with a thickness of up to approximately 14.0 m, and prestressed pipe pile was selected for reinforcing the soft soil foundation to increase bearing capacity and reduce settlement. Embankment sliding with a length of approximately 110 m and cracking with a length that exceeded 300 m occurred before the construction of the pavement structure. Field investigation and theoretical analysis results indicate that the safety factor of the overall stability calculated by the existing code methods is overly large, thereby resulting in large design pile spacing, low design bearing capacity provided by single pile, and excessive load shared by subsoil between piles. These results all cause the flow sliding of soft soil between the piles and the bending fracture of some piles. The revised density method can be used to check the stability of flow sliding, and the bending moment of piles should also be checked during the embankment design stage. In addition, perpendicularity deviation and poor joint quality of pile construction also contributed to the reduction of the bearing capacity of the pipe piles and the overall stability of embankment. Reconstruction of additional rigid piles and add pile after drilling holes are adopted in the sliding and cracking sections to reinforce the failed embankment, respectively. The remediation effect was validated by the measured excess pore water pressure, subgrade settlement, and horizontal displacement.

1. Introduction

In recent decades, several expressways and high-speed railways were constructed in coastal areas with deep soft soil, which possesses low shear strength and high compressibility. With the increase in soft foundation treatment depth, embankment height, and postconstruction settlement requirement, rigid columns (e.g., prestressed pipe pile, cement fly-ash gravel pile, and concrete pile) have been widely used to strengthen the soft foundation and form a composite foundation to support the embankment because of its fast construction speed and reliable settlement control effect [1–3]. Most rigid-pile composite foundation supports embankment successfully; however, accidents, such as collapse, cracking, and excessive settlement of embankments, occur in some areas [4–9].

The limit equilibrium method is generally adopted in the current specifications of China for the stability analysis of embankment supported on the rigid-pile composite foundation [10, 11]. The shear failure of soil and pile occurs along the circular sliding surface, and the overall stability is analyzed according to the composite shear strength of soil and pile. However, many researchers emphasized that, in addition to pile shear failure, the failure modes of rigid pile under embankment include pile bending failure, pile inclination, pile compression failure, and soil flow around pile. Zheng et al. [12, 13] investigated the influence of the bending capacity of rigid pile on the stability of embankment through centrifugal test and numerical analysis. The research shows that the bending fracture is the main failure mode of the rigid pile in embankment, the progressive failure of rigid pile occurs, and the effect of rigid pile on the stability of embankment in different parts varies. Kitazume et al. [14]

discovered the bending failure of the pile under the embankment through the centrifugal model test. The British code [15] introduced the stability calculation method of geosynthetic-reinforced pile-supported embankment. The vertical bearing capacity of the pile under the sliding surface is considered the axial supporting force of the sliding body rather than the shear strength of the pile. This method essentially aims to analyze the stability of soil flow around a pile and not the overall stability of the embankment. Liu et al. [16, 17] proposed a modified density method that could be used to analyze the stability of rigid-pile composite foundation by using the existing conventional stability analysis software of subgrade based on the flow failure mode of the embankment on the rigid-pile composite foundation. In this method, the friction around the pile is converted into the medium weight of the foundation soil in the reinforcement area by reducing the embankment load to calculate the safety factor of flow sliding. Wang et al. [18] studied the lateral response of a single precast concrete pile reinforced with cement-improved soil based on theoretical studies and 3D finite element analyses. Although many useful researches for failure mode and stability calculation method of rigid-pile composite foundation have been reported, studies on the analysis of the causes of the failed embankment over the rigid-pile composite foundation and the discussion on the effect of the remediation measures are limited.

A failed embankment on prestressed pipe-pile-improved soft soil in Guangdong Province, China, has been reported and analyzed in this paper. The geotechnical properties, embankment geometries, soft foundation treatment method, and construction history at the site, as well as the embankment failure event, are initially described briefly. Then, the reasons for the failure of embankment sliding and cracking are analyzed on the basis of field investigation and theoretical analysis. Finally, the remediation measures and reinforcement effect are presented and discussed.

2. Site Conditions and Project Overview

2.1. Embankment Diseases. Figure 1 shows the location of the South Extension Project of Xintai Expressway. This project is located in Doushan, Taishan City, Guangdong Province, China. Its total length is approximately 5.7175 km. After a rainstorm, the constructed embankment exhibited some failures in different sections [19]. Two classic failure sections (e.g., the cracking section: K63 + 500~K63 + 710; the sliding section: K64 + 080~K64 + 180) were selected for the following research.

The cracking section is located in the alluvial plain, and some fish ponds are distributed on both sides of embankment. During the embankment unloading process, the embankment had evident macroscopic deformation, and several large cracks had appeared on both sides of the drainage ditches. The right drainage ditch was dislocated by 6–18 mm, cracked by 3–12 mm, and sunk by 5–11 mm.

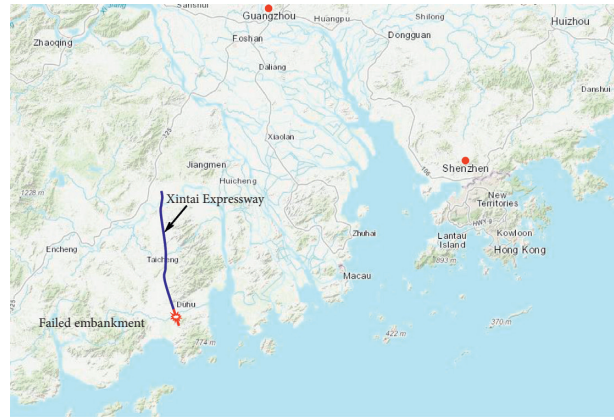

Figure 1: Location of failed embankment.

The sliding section is located in the bridge approach, and the embankment is surrounded by farmland. After the embankment construction was completed, the right and left embankments slid successively (Figure 2). The length, width, fill height, maximum ground-lifting height, and ground-lifting width of the right sliding embankment are approximately 110 m, 10 m, 6.9 m, 2.177 m, and 17.3 m, respectively, whereas those of the left sliding embankment are 110 m, 8 m, 6.9 m, 2.021 m, and 26.2 m, respectively (Figure 3).

2.2. Geological Conditions. This expressway runs through coastal alluvial plains and hilly areas, in which the upper layers are composed of Quaternary Holocene tillage soil, alluvial silty clay, silt, sandy soil, mud soil, muddy clay, and muddy sand. We have selected K63 + 500 from the cracking section and K64 + 080 from the sliding section to analyze and have an accurate study on embankment diseases. The physical and mechanical parameters of each soil layer are shown in Tables 1 and 2, respectively.

2.3. Design and Construction. The width and slope of this embankment are 24.5 m and 1 : 1.5, respectively. PHC300A70 was adopted to treat the soft soil foundation, the pile cap size is 1.5 × 1.5 × 0.35 m, and the layout of the pipe piles is rectangular or square. The plastic drainage plates with the same spacing as those in pipe piles were set in section K64 + 120–K64 + 180. Table 3 demonstrates the design parameters of the embankment and pipe piles. In addition, 35 cm medium coarse sand among pile caps and 30 cm gravel cushion were laid above the pile caps. Two layers of biaxial geogrid were paved on the upper and lower sides of the gravel cushion, which has an ultimate tensile strength of not less than 50 kN/m. Before the occurrence of embankment diseases, the completed or ongoing construction procedures are presented as follows: plastic drainage plates ⟶ prestressed pipe piles ⟶ pipe caps ⟶ sand cushion ⟶ gravel cushion ⟶ lower embankment ⟶ upper embankment ⟶ lower roadbed.

(a) (b) (c)

Figure 2: Sliding failure of the embankment. (a) Sliding of the left embankment. (b) Sliding of the right embankment. (c) Excavation investigation.

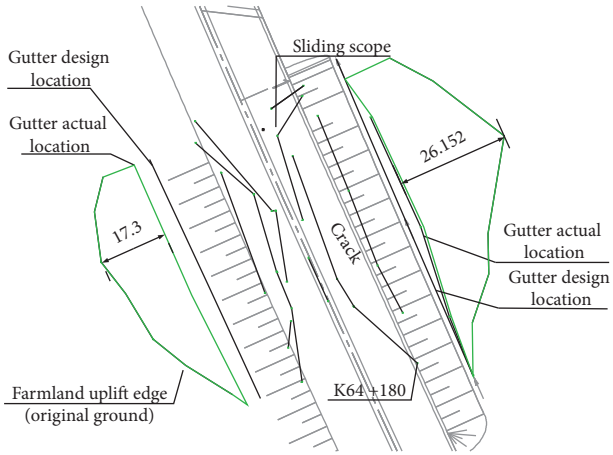

Figure 3: Schematic plan of the embankment in the sliding section.

3. Reason Analysis of Sliding and Cracking

3.1. Unreasonable Calculation Method of Stability. In rigid-pile composite foundation, the general shear failure of soil and rigid piles along the sliding surface merely occurs. Many studies have shown that the flow sliding of soft soil mainly occurs between piles in composite foundation (Figure 4). Flow sliding causes the occurrence of bending fracture or inclination, but not shear fracture, in the pipe piles. The safety factor (F_s) of embankment, which is calculated according to general shear failure theory, is too large to be consistent with the actual project. However, most of the present standards are still based on this theory. Thus, many potential dangers are hidden in the design phase.

Embankment stability can be calculated using four methods. Method 1 refers to the method specified in *Technical Guidelines for Design and Construction of Highway Embankment on Soft Ground* [15]. Methods 2 and 3 are described in *Technical Code for Ground Treatment of Buildings* [11]. Method 4 is a new method proposed by Liu et al. [16, 17]. In summary, although these four methods are all based on limit equilibrium theory, they still have differences. Methods 1, 2, and 3 are included in the present specifications for calculating the safety factor under general shear failure. However, different assumptions and calculation methods are followed. Method 4 is used to calculate the safety factor under the flow sliding failure. The following is a brief introduction to the four methods:

Method 1: in accordance with the standard of *Technical Guidelines for Design and Construction of Highway Embankment on Soft Ground* [15], the composite shear strength of composite foundation is calculated by the area-weighted of piles and soil:

$$\tau_{ps} = m\tau_p + (1 - m)\tau_s, \quad (1)$$

where m is the area replacement rate of pile; τ_p is the composite shear strength of the composite foundation; τ_p is the shear strength of pile; τ_s is the undrained shear strength of soil between piles; and the shear strength of the pile is 0.5 times of its compressive strength.

Method 2: *Technical Code for Ground Treatment of Buildings* [11] considers that the overall sliding of piles and soil occurs after the piles bending fracture. When analyzing the stability of embankment, the cohesion of concrete (c_c) is 0 kPa and the friction angle (φ_c) is 35°. The composite shear strength of the composite foundation is also calculated by equation (1), and the friction angle of the composite foundation is calculated by using the following equation:

$$\tan\varphi_{sp} = R_s \tan\varphi_s + (1 - R_s)\tan\varphi_c, \quad (2)$$

where φ_{sp} is the composite friction angle, φ_s is the friction angle of soil between piles, φ_p is the friction angle of concrete, and R_s is the load rate of soil between piles.

Method 3: according to the "sand pile" method mentioned in the *Technical Code for Ground Treatment of Buildings* [11], the rigid piles are assumed to be equivalent to the sand piles with a certain friction angle. The friction angle is determined by the friction factor of

Table 1: Physical and mechanical parameters of each soil layer in section K63 + 500.

Soil	h (m)	w (%)	γ (kN/m^3)	E_s (MPa)	c_q (kPa)	φ_q (°)	$K_v/10^{-8}$ cm/s	q_c (MPa)	f_s (kPa)
Silty clay	1.2	42.6	16.5	2.6	3.9	4.9	41.6	3.0	47.1
Silt	8.4	75.5	17.2	8.4	5.8	4.0	13.3	0.3	5.2
Silty clay	2.3	47.9	17.0	2.3	4.5	4.9	34.1	1.3	36.0
Silty medium sand	2.2	20.3	16.8	2.2	13.4	11.2	108.7	5.0	48.0
Silty clay	5.1	75.8	15.9	1.8	7.1	7.2	34.6	4.9	22.6
Completely decomposed granites	3.2	—	19.2	—	20.0	20.0	—	10.9	44.5

Note: w = water content; γ = natural weight; E_s = modulus of compressibility; c_q = cohesion (from quick direct shear test); φ_q = internal friction angle (from quick direct shear test); K_v = permeability of the soil in the vertical direction; q_c = static point resistance; f_s = side friction.

Table 2: Physical and mechanical parameters of each soil layer in section K64 + 080.

Soil	h (m)	w (%)	γ (kN/m^3)	E_s (MPa)	c_q (kPa)	φ_q (°)	$K_v/10^{-8}$ cm/s	q_c (MPa)	f_s (kPa)
Planting soil	0.6	28.0	18.0	3.6	8.0	16.0	68.3	2.6	52.0
Silty clay	0.6	42.6	16.5	2.6	3.9	4.9	41.6	1.1	35.7
Silt	4.6	67.5	16.2	2.0	4.8	4.8	15.3	0.1	3.4
Silty fine sand	1.9	35.7	18.9	3.8	16.4	10.4	96.7	2.1	11.2
Silt	8.5	78.5	18.2	2.6	8.8	3.7	26.9	0.4	4.0
Silty clay	3.0	23.5	20.6	3.6	6.5	7.2	30.5	3.9	16.6

Table 3: Design parameters of the embankment and prestressed pipe pile.

Section	Embankment type	Filling height (m)	Pile lateral spacing (m)	Pile longitudinal spacing (m)	Pile length (m)
K64 + 080	Bridge approach	7.17	2.6	2.6	19
K64 + 100	Transition	7.10	2.6	2.8	19
K64 + 120	Normal	7.00	3.0	3.0	18
K64 + 160	Normal	6.74	3.0	3.0	18

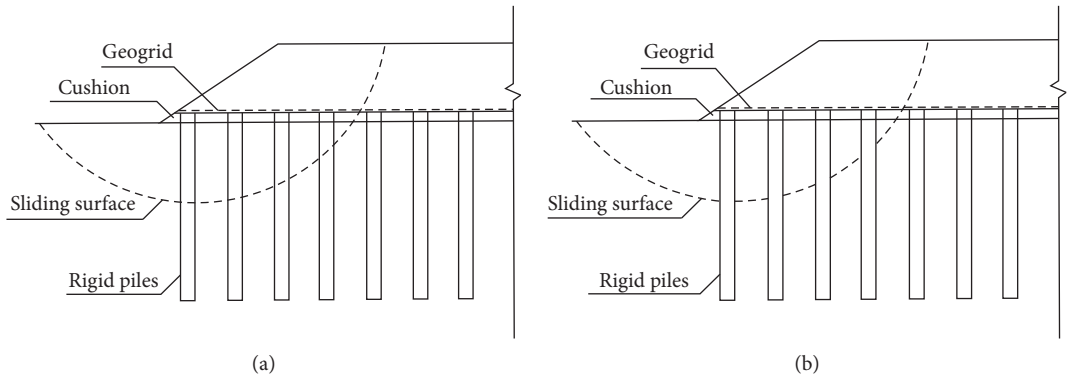

Figure 4: Schematic diagram of general shear failure and flow sliding failure. (a) General shear failure. (b) Flow sliding failure.

the pile material after the bending failure, the pile-soil stress ratio is taken as 3, and the composite internal friction angle is calculated by using the following equation:

$$\tan\varphi_{sp} = \frac{(1-m)\tan\varphi_s + mn\tan\varphi_c}{1-m+mn}, \quad (3)$$

where m is the area replacement rate of pile and n is pile-soil stress ratio.

After calculating the composite parameters by using Methods 1, 2, and 3, respectively, we can use the natural pile-free foundation using the aforementioned composite parameters instead of the actual prestressed pipe-pile composite foundation to calculate the safety factor by using some embankment stability analysis software.

Method 4: revised density method Liu et al. [16, 17] is different from the existing normative methods. It is used to calculate the stability of embankment flow sliding, which considers the embankment filling and soil between the piles as the analysis objects. In Figure 5, the soil above the sliding surface receives three forces from the pipe piles: the vertical force on top of the pile cap P_p, the friction force of soil between piles τ, and the horizontal force of soil among the piles q_h. These three forces can prevent the

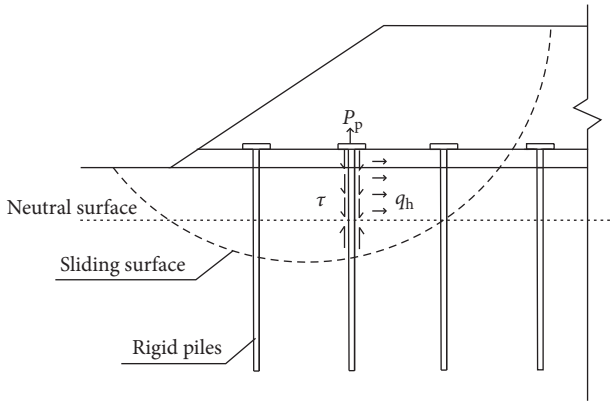

Figure 5: Forces exerted by pipe piles on sliding soil.

occurrence of flow sliding failure. However, q_h that the pipe pile can withstand is very small because the cracked resistant bending moment of pipe pile is very small. Engineers usually ignore it during the design process to increase project safety. Thus, P_p and τ become the main factors for improving embankment stability. We can use the modified densities to replace the effect of P_p and τ by utilizing the revised density method. Thus, the revised densities should be adopted in the embankment and reinforced foundation soils, the original density should be adopted to the soil outside the reinforcement area, and unrevised shear strength should be adopted to the embankment soil (Figure 6). Then, similar to the three aforementioned methods, we can use the conventional stability analysis software to calculate the safety factor based on limit equilibrium theory.

The calculation steps of Method 4 are presented as follows: calculate the top load $P_p \longrightarrow$ determine the location of neutral surface $\longrightarrow$ calculate revised densities and revise shear strength indexes of soil between piles $\longrightarrow$ check the stability of composite foundation with flow sliding $\longrightarrow$ check the stability of embankment filling with flow sliding. The following is the detailed description of the aforementioned calculation steps.

P_p shall take the minimum of $F_s P_{pa}$ and Q_{uk} (the standard value of vertical ultimate bearing capacity of single pile), F_s adopts the method mentioned in the [15] for calculation, P_{pa} can be calculated by the improved HEWLETT method proposed by Chen et al. [20], and Q_{uk} can be calculated by the following equation according to the data of Cone Penetration Test (CPT):

$$Q_{uk} = u_p \sum \beta_i f_{si} \Delta z_i + \alpha_b A_p q_c, \tag{4}$$

where u_p is the perimeter of pile, β_i is the comprehensive correction coefficient of the ultimate friction resistance of layer soil i, f_{si} is average lateral friction of layer soil i, Δz_i is the thickness of the layer soil i, α_b is the comprehensive correction coefficient of the ultimate bearing capacity of the pile end, A_p is the area of the pile end, and q_c is the pile tip resistance.

The upper and lower areas of the piles are divided into negative and positive friction zones, and the interface of the two zones is called the neutral surface because of the different settlements between piles and soil among piles. The location of neutral surface can be determined by using the following equation:

$$Q_s^n = \frac{Q_{uk} - P_p}{2}. \tag{5}$$

The revised density of the embankment filling above the pile caps ρ_{fr} and the embankment soil between piles ρ_{fdr} can be revised by using equations (6) and (7), respectively:

$$\rho_{fr} = F_s \rho_f \frac{F_s P_u - P_p}{F_s P_u}, \tag{6}$$

$$\rho_{fdr} = F_s \rho_{fd} (1 - m) + \frac{u_p \tau}{D^2 g}, \tag{7}$$

where ρ_f is that design density of embankment soil, ρ_{fd} is that design density of embankment soil between piles, P_u is that load above the top of pile cap within the shared area of single pile, m is that area replacement rate of piles, u_p is that perimeter of pile, τ is that friction force of soil between piles (negative friction force is taken as negative value), D is that pile spacing, and g is that gravity acceleration.

The revised soil density in the reinforced area ρ_{sr} should be calculated according to

$$\rho_{sr} = \rho_s (1 - m) + \frac{u_p \tau}{d^2 g}. \tag{8}$$

When pipe piles do not penetrate the soft soil layer, the revised density of the soil at the pile end area ρ_{sr} shall be calculated by using the following equation:

$$\rho_{sr} = \rho_s + \frac{Q_{pk}}{d^2 T_e g}, \tag{9}$$

where ρ_s is the design density of soil between piles; Q_{pk} is the standard value of total ultimate pile end resistance; and T_e is the thickness of the pile end area, which can be taken as 0.5–1.0 m.

Cohesion c and undrained shear strength of soil between piles C_u can be revised according to equations (10) and (11), respectively. The internal friction angle φ of soil between piles need not be revised because the quality of soil between piles is constant.

$$c_r = c(1 - m), \tag{10}$$

$$C_{ur} = C_u (1 - m), \tag{11}$$

where c_r is the revised cohesion and C_{ur} is the revised undrained shear strength.

The comparison among the safety factors calculated by the four aforementioned methods is shown in Table 4. The results of the revised density method can conform to the actual situation of this project remarkably, whereas the calculation results of the three other methods specified in the standards vary slightly from the actual situation, especially

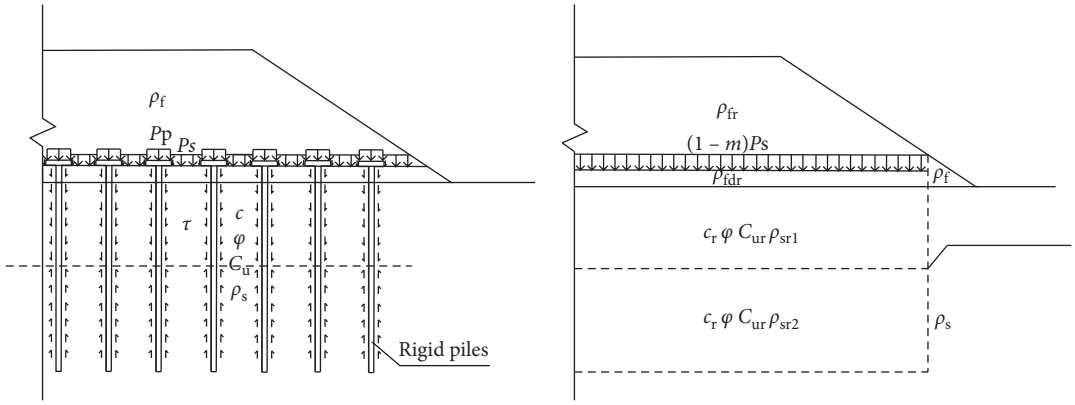

Figure 6: Schematic of the revised density method. (a) Original embankment. (b) Revised embankment.

the results in Method 1, which are too large, thereby resulting in a huge hidden danger in the design process.

The data of settlements and bending moments on the sliding section and the cracking section are included in Table 5. The maximum bending moment M_{max} of the pipe piles on the checking section is generally larger than the ultimate bending moment M_u, because the present standards do not require the calculation of the bending capacity of piles. This design negligence causes the design bending capacity of the pipe pile to be small, thereby making the pipe piles prone to the occurrence of bending fracture under the embankment load, and reduces the overall stability of embankment.

According to the settlement data in Table 5, the settlements of all monitoring sections are larger than the specified value, which will also have a negative impact on embankment stability. The stability checking methods in the existing standards usually overestimate embankment stability, which will lead to larger pile spacing and small designed bearing capacity of single pile in the design process. Thus, in the actual construction, the bearing capacity of the composited foundation could not support the upper load well, and the load shared by the soil between piles becomes too larger to maintain small deformation and hence the occurrence of excessive settlement.

3.2. Influence of Perpendicularity Deviation. In order to study the influence of the perpendicularity deviation, engineers set up the inclinometer into the pipe pile, measured the deviation of pile top to bottom, and obtained the perpendicularity deviation of pipe pile. Figure 7 shows the statistical figure of the perpendicularity deviation of pipe pile obtained from 33 monitoring piles. All perpendicularity deviations exceed 0.5%, which is the allowable value for the prestressed pipe pile, and most of the monitoring values are concentrated in 0.5%–3.5%, indicating that the excessive perpendicularity deviation is a nonnegligible factor of embankment diseases.

The influences of perpendicularity deviation on pipe piles are mainly manifested in two aspects: overturning and bending stability. We can analyze the influences based on the bearing capacity of single pile. Figure 8 shows the value of the ultimate bearing capacity of single pile Q_{uk}. When analyzing the influence of perpendicularity deviation on the overturning stability, we need to make the following assumption: the soil between piles is considered soft soil, and when piles overturn, the pipe piles are subjected to the active earth pressure ρ_a from one side soil and the passive earth pressure ρ_p from the other side (Figure 9).

According to the moment balance condition of piles (equation (12)), we can enable equation (13) to calculate the vertical load on the pile top controlled by the overturning stability of the pile (P_p').

$$iP_pL = 2C_u dL^2, \tag{12}$$

$$P_p' = \frac{2C_u dL}{i}, \tag{13}$$

Table 4: Comparison of safety factors calculated by using the four methods.

Section	Method 1	Method 2	Method 3	Method 4
K64 + 080	2.619	1.606	0.697	0.976
K64 + 100	2.638	1.573	0.698	0.951
K64 + 120	2.446	1.632	0.865	1.281
K64 + 160	2.515	1.380	0.753	0.959

Table 5: Statistical table of settlements and bending moments.

Section	Settlement (mm)	M_{max} (kN·m)	M_{max}/M_u
K63 + 505	754.9	195.7	5.28
K63 + 540	394.1	81.2	2.19
K63 + 560	533.8	84.3	2.28
K63 + 620	586.3	176.9	4.78
K63 + 700	694.2	206.0	5.56
K64 + 080	1579.5	76.3	2.06
K64 + 100	868.1	46.4	1.25
K64 + 120	1088.3	56.1	1.52
K64 + 160	1897.7	93.6	2.53

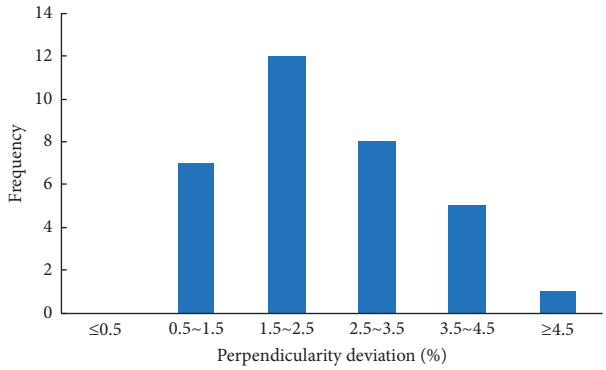

Figure 7: Sectional statistics of vertical deviation of pipe pile.

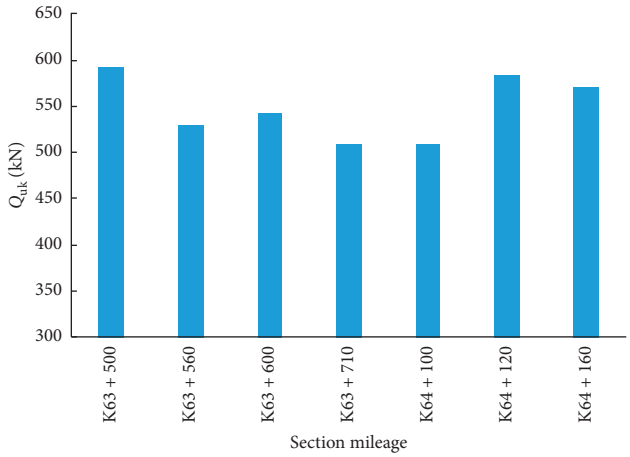

Figure 8: Histogram of Q_{uk} in different sections.

where P_p is vertical load on the pile top, P_p' is the vertical load on the pile top controlled by the overturning stability of the pile, L is the pile length, i is the perpendicularity deviation, C_u is the undrained shear strength of the soft soil, and d is the pile diameter.

In this work, $i_{max} = 6.5\%$, $L_{min} = 15$ m, $Cu_{min} = 7.3$ kPa, and $d = 0.3$ m. Thus, we can calculate $P_p' = 1010.8$ kN, which is the minimum value of the vertical load on the pile tops that makes the pipe pile overturn. According to the revised density method, P_p is the minimum of $F_s P_{pa}$ and Q_{uk}. Therefore, $P_p < Q_{uk}$. Figure 8 shows that P_p' is less than Q_{uk}; that is, $P_p' < P_p$. Therefore, the impact of the pile's perpendicularity deviation on the bearing capacity of the single pile will not cause the piles to overturn.

The influence of perpendicularity deviation on bending moment is presented as follows.

Based on equations (14) and (15), we can enable equation. (16) to calculate the vertical load on the pile top controlled by the ultimate bending moment of the pile P_p''; that is, when the load on the pile top exceeds the value of P_p'', the bending moment of the pile will reach the maximum value, and the pile will be damaged.

The bending moment of the piles at depth z is as follows:

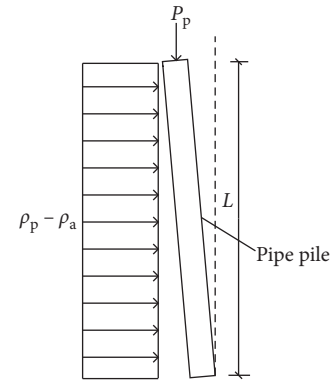

Figure 9: Stress on pile when overturning.

$$M = izP_p - 2z^2 C_u d, \tag{14}$$

$$M_{max} = \frac{i^2 P_p^2}{8 C_u d}, \tag{15}$$

$$P_p'' = \frac{2}{i}\sqrt{2 M_u C_u d}. \tag{16}$$

In this project, $i_{max} = 6.5\%$, $L_{min} = 15$ m, $Cu_{min} = 7.3$ kPa, $d = 0.3$ m, and $Mu = 37$ kN·m (the minimum ultimate bending moment of PHC300A70, from *Technical Code for Building Pile Foundations (JGJ94-2008)*). Thus, we can calculate $P_p'' = 391.7$ kN by using equation (16), indicating that the maximum pile top load that the pipe pile can bear is 391.7 kN. This value is smaller than that of Q_{uk} in Figure 8. Therefore, perpendicularity deviation could reduce the actual bearing capacity of the single pile and result in the bending failure of the pipe pile under large upper load.

From the aforementioned analysis, we can conclude that the bearing capacity of the single pile may be reduced because of excessive perpendicularity deviation, which leads to the penetration failure at the pile end and affects the stability of embankment. In addition, if the perpendicularity deviation of adjacent pipe piles is in an opposite direction, then the pile spacing will be expanded further, thereby reducing the soil arching effect on the pile top so that considerable embankment load will be transferred to the soil between piles, which will also result in excessive soil load and settlement of foundation among piles.

3.3. Influence of Poor Joint on Pipe Pile. The depth of soft soil bottom at the sliding section is approximately 14 m, and the length of the pile is 18-19 m. Each pile consists of two identical prefabricated piles. Thus, the joint of the two piles is located in the middle of the soft soil layer, in which the maximum positive moment of piles is located. In detecting the integrity of piles on the diseased section, the defect locations of piles usually occur near the joint. Figure 10 shows the interior pipe-pile monitoring result obtained by hole camera technology. Dislocation and water leakage have occurred at the joints of some pipe piles.

The pile concrete on the potential sliding surface is subjected to not only compressive stress but also shear stress parallel to the potential sliding surface. Thus, before the pile exhibits shear failure along the sliding surface, it has been destroyed in other directions under the action of the two aforementioned stresses. Therefore, Miao et al. [21] defined shear strength to analyze the failure mechanism of concrete piles more reasonably, and the occurrence of shear strength can be calculated by two criterions, maximum tensile stress criterion and Mohr–Coulomb criterion. When the shear stress of the concrete pile on the potential sliding surface is larger than the shear strength determined by maximum tensile stress criterion, the concrete pile exhibits tensile failure along direction β. When the shear stress of the concrete pile on the potential sliding surface is larger than that determined by the Mohr–Coulomb criterion, the concrete of the pile shaft shears along direction ψ. Figure 11 demonstrates the relationship of the three aforementioned directions in piles.

The shear and tensile failure surfaces of concrete pile are similar to the No. 2 or even No. 3 group of joint surfaces in rock. The shear strength on potential sliding surface will not be affected as long as their directions are different from the sliding surface. Embankment does not move and slide even if the piles have broken because the actual fracture surface of the concrete pile is inconsistent with the direction of the potential sliding surface. However, the potential failure surface affects the distribution of the bending moment on the pile when the cracks penetrate the entire pile. It also influences the vertical bearing capacity of the single pile when the title angle of the failure surface in the pile is larger than its internal friction angle.

Therefore, although the poor joint in the pipe pile is not the main factor that causes embankment diseases, it reduces the bending bearing capacity of pipe pile and causes the pipe pile to be prone to bending failure.

Figure 10: Pipe-pile joint monitored by camera technology in the hole.

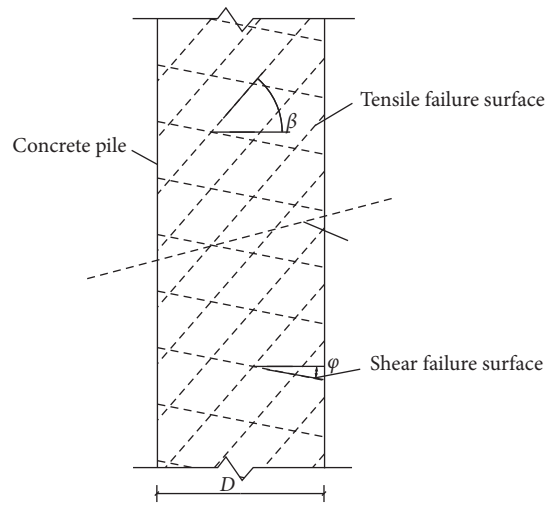

Figure 11: Relationship between sliding surface and actual failure surface.

4. Remediation Measures and Effect Analysis

4.1. Remediation Measures. After embankment slid, plenty of reinforcement measures were applied to the sliding and other sections. Engineering monitoring was also valued during and after construction. This paper mainly introduces and analyzes the reinforcement measures on the sliding and cracking sections. The cross sections and plans of reinforcement measures at the two sections are shown in Figure 12.

4.1.1. Cracking Section. Add piles after drilling holes (APDHs) were applied for the reinforcement of the diseased composite foundation. However, we need to unload 2 m thickness embankment soil first. The add piles adopted PHC400A95; the length and pile spacing are 24 m and 2.8 m, respectively. The pile end must be closed to make it a fully squeezed pile. After determining the locations of the old pipe piles, long spiral rod must be used to drill holes to the bottom of the gravel cushion at the center of the four adjacent original piles. Then, the add piles were drilled in the drilled holes. Finally, the microexpansion concrete C20 filled the top of the embankment. Figures 12(a) and 12(c) present the cross section and plan of remediation measures in the cracking section.

4.1.2. Sliding Section. Reconstructed pipe piles, plastic drainage plates, and loading berms were applied to reinforce this section. First, the damaged and inclined pipe piles were cleared after moving the remaining soil above the original supporting plate. Second, a 30 cm working cushion was laid, and plastic drainage plates were constructed. Third, the reconstructed pipe piles were laid down among the original pile caps, and 50 cm gravel cushion was placed above the pile caps. The spacing of the reconstructed pipe piles is similar to that of the original pile, and their length is 23 m. Finally, the loading berm was set on both sides of the new embankment. Figures 12(b) and 12(d) show the cross section and plan of remediation measures in the sliding section.

4.2. Monitoring Scheme. During the construction of remediation measures, meaningful monitoring actions, including excess pore water pressure, subgrade settlement, and

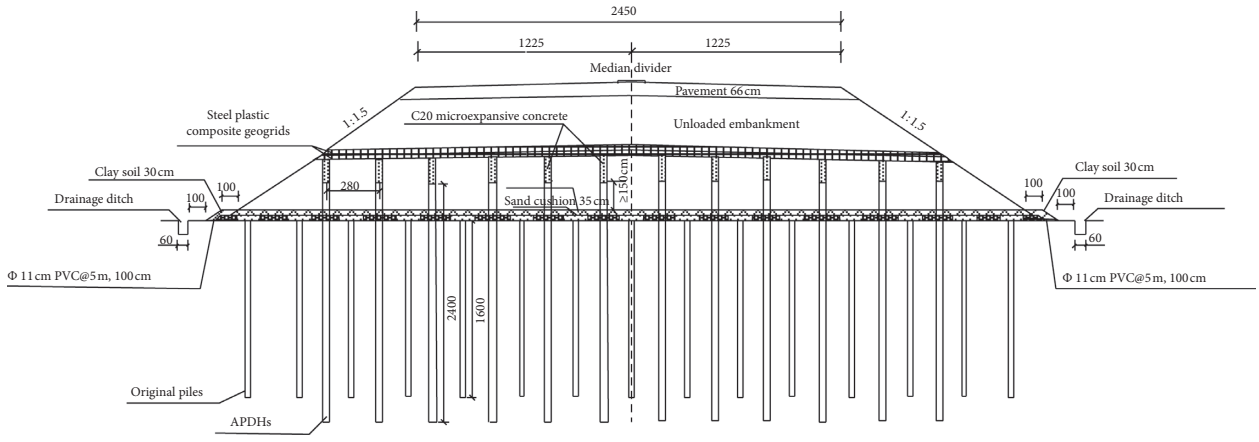

(a)

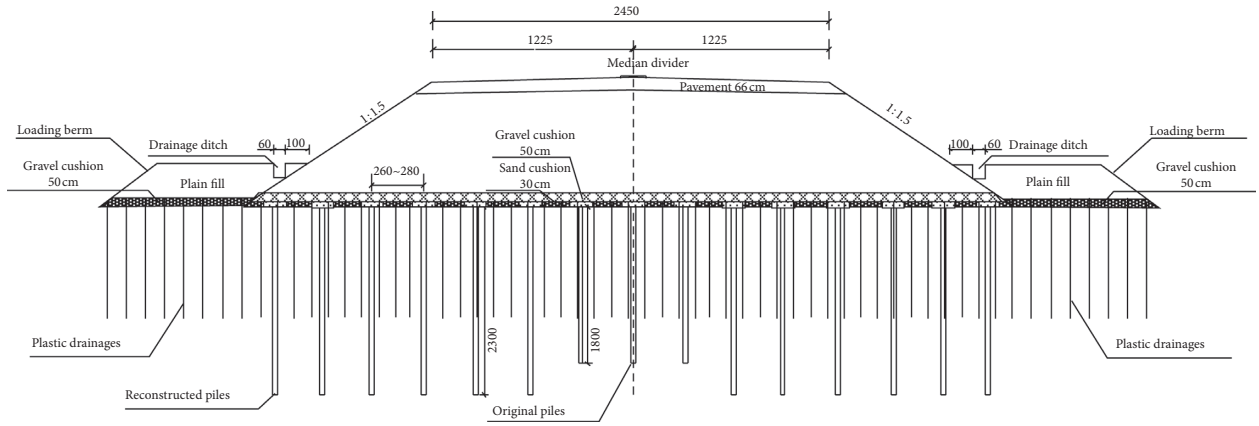

(b)

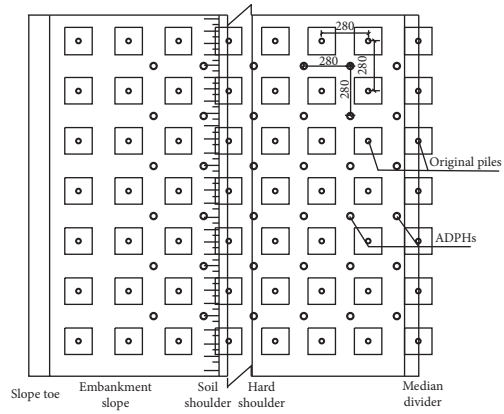

(c)

Figure 12: Continued.

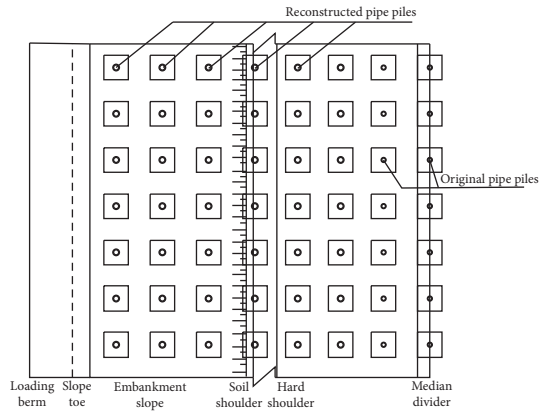

Figure 12: Cross sections and plans of reinforcement measures in two sections. (a) Cross section of the cracking section. (b) Cross section of the sliding section. (c) Plan of the cracking section (half embankment). (d) Plan of the sliding section (half embankment).

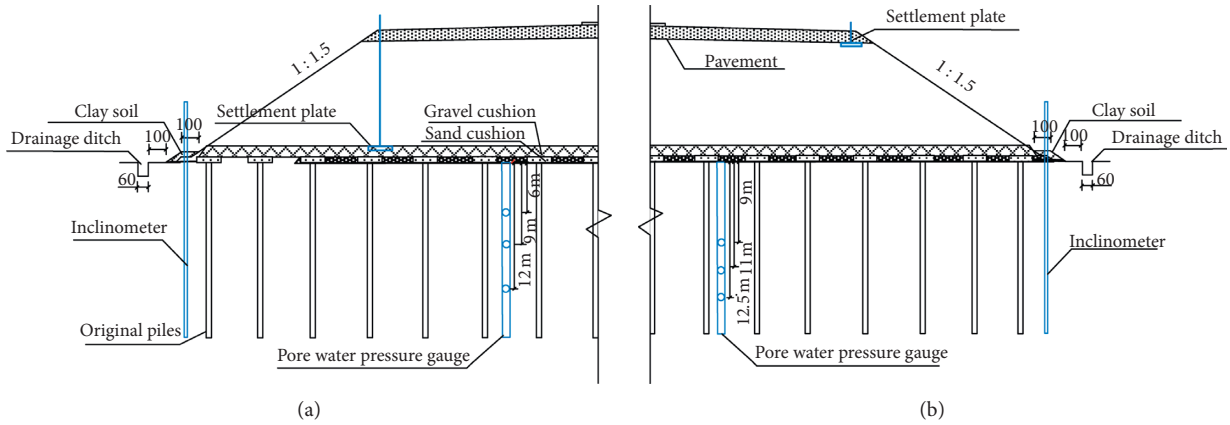

Figure 13: Schematic of the monitoring section. (a) Sliding section. (b) Cracking section.

horizontal displacement, have been applied to the remediated embankment to analyze the remedy effect [22].

The excess pore water pressure could be monitored by the pore water pressure gauges. Six pore water pressure gauges are buried in the both sides of the foundation. One side has three gauges buried in different depths (cracking section: 6 m, 9 m, and 12 m; sliding section: 9 m, 11 m, and 12.5 m). Subgrade settlement could be monitored by the settlement plate and settlement monitor mark. Three settlement plates or settlement monitoring marks are placed in the center of the embankment and the left and right shoulders. Two inclinometers are buried at the foot of the embankment to monitor the horizontal displacement data. Figure 13 shows the schematic of the monitoring section in two remedial sections. The left part refers to the sliding section while the right part corresponds to the cracking section.

4.3. Reinforcement Effect in Cracking Section. In the cracking section, the monitoring data of section K63 + 500 are taken as examples to analyze the reinforcement effect, and the results of other sections are similar to that of section K63 + 500.

Excess pore water pressure P_w is an important factor that should be considered in the design and construction of pipe-pile composite foundation. The soil will be remolded partially in the 1-2 times of the area of the pile diameter when the piles were drilled. Thus, the pore water pressure subjected by soil may reach or even exceed the overlying pressure. Figure 14 shows the variation curves of pore water pressure with filling load in section K63 + 500 since the construction of the reconstructed piles. During the construction of the reconstructed piles, the composite foundation produced large excess pore water pressure in a short time because of the fast construction speed of piles and concomitant soil squeezing effect. After the completion of pipe-pile construction, the pore water pressure began to dissipate gradually, but the deepest pressure dissipated most slowly because this measuring point is located at the bottom of the silt layer with low permeability. During the construction of embankment, the pore water pressure has changed slightly, showing that the pore water pressure in the pipe-pile composite foundation is basically stable under small embankment load. This finding proves that the bearing capacity of the new pipe-pile composite foundation is better, the load of soil between piles is smaller, and the embankment

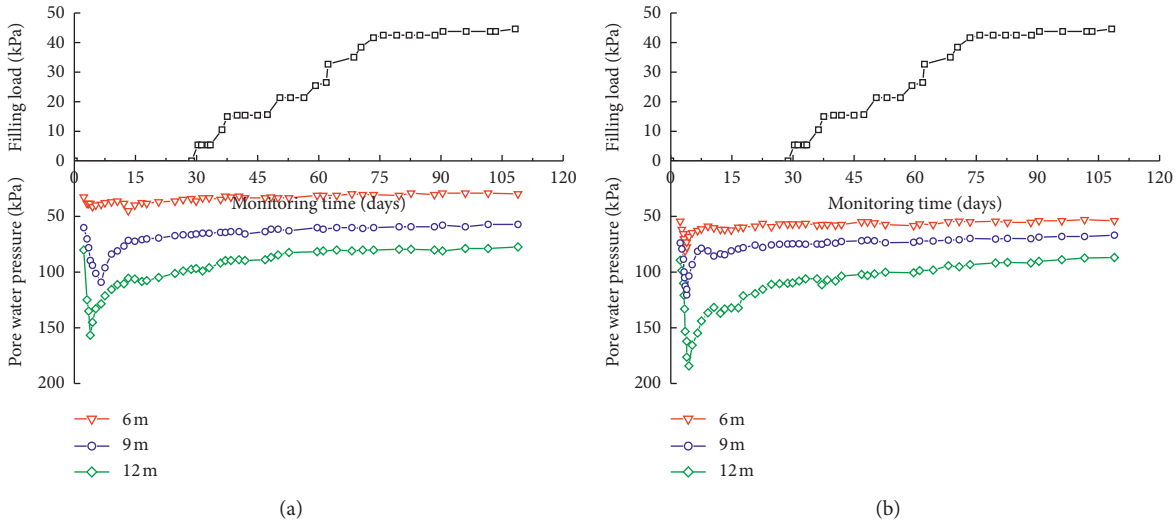

Figure 14: Variation of pore water pressure with filling load. (a) Left embankment. (b) Right embankment.

is more stable than before. Therefore, continuous filling with small load can also ensure the stability of the embankment when the external construction conditions are suitable.

The settlements should be observed dynamically during the construction of the expressway on soft soil foundation. According to the observation data, engineers can adjust the embankment filling rate and predict the later settlement rate and the overall stability of embankment. Figure 15 shows the variation curve of cumulative settlement with filling load since the construction of APDHs. The soil squeezing effect causes the ground to uplift greatly because of the construction of APDHs. During embankment filling, the settlement of the foundation gradually increases, but the settlement rate gradually decreases until it becomes basically stable. The comparison of the settlements before and after reinforcement shows that the settlement of foundation can be reduced effectively by the reinforcement of APDHs.

With the development of foundation settlements, the embankment stress is redistributed, and the soil arching effect is affected. The horizontal, vertical, and shear stresses near the toe of the slope will increase. The horizontal displacements and additional settlements will appear with the development of embankment plastic zone, and the embankment instability will appear and develop further, unless the timely monitoring was not carried out. Figure 16 shows the cumulative horizontal displacement curve of section K63 + 500 in different construction stages, and Figure 17 shows the variation of the maximum horizontal displacement with filling load in the left section K63 + 500.

In Figure 16, the horizontal displacement increased evidently when the APDHs are constructed, which proves the soil squeezing effect. Thereafter, the horizontal displacement has a slight rebound because of the dissipation of pore water pressure after the completion of APDH construction. With the completion of embankment and pavement, the horizontal displacement gradually stabilized because the pore water pressure value is basically stable, and the deformation and movement of soil skeleton particles

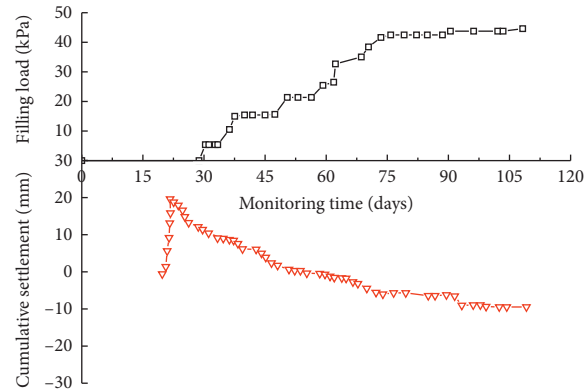

Figure 15: Variation of cumulative settlement with filling load.

have been completed. In Figure 17, the maximum cumulative lateral displacement has a significant increase before the embankment was built, that is, the period of the construction of APDHs. However, during the embankment filling, the maximum cumulative lateral displacement remains stable despite the increase in filling height, indicating that the use of APDHs to reinforce failure foundation can improve the bearing capacity of foundation and constrain the development of lateral displacement. However, from the construction standpoint, we need to pay more attention to the soil squeezing effect and the construction rate of APDHs and avoid the occurrence of foundation instability.

4.4. Reinforcement Effect in Sliding Section. In the sliding section, we take the monitoring data of section K64 + 080 as the analytical section to evaluate the reinforcement effect.

Figure 18 shows the variation curves of pore water pressure with filling load for the left embankment in section K64 + 080. The variation of pore water pressure during the construction of the pipe pile is similar to that in section K63 + 500. In the monitoring time of 35 days, the pore water pressure increased slightly due to the fast embankment

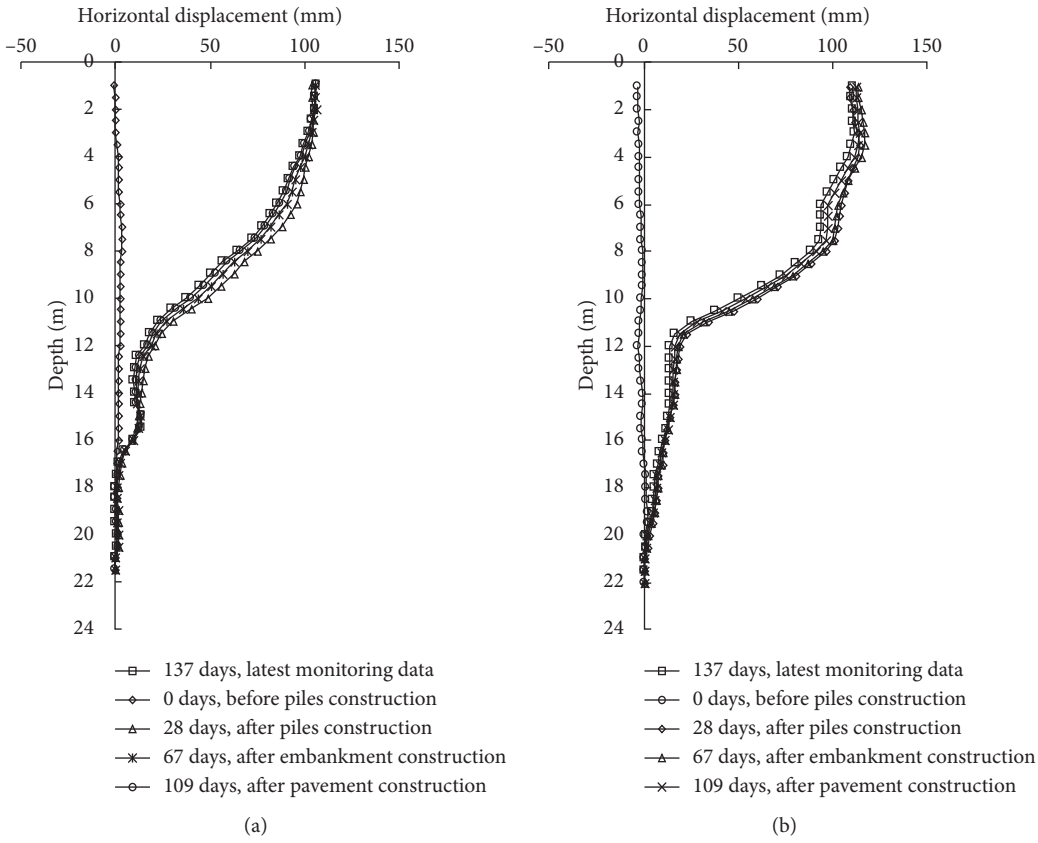

Figure 16: Variation of cumulative horizontal displacement in different construction stages. (a) Left embankment. (b) Right embankment.

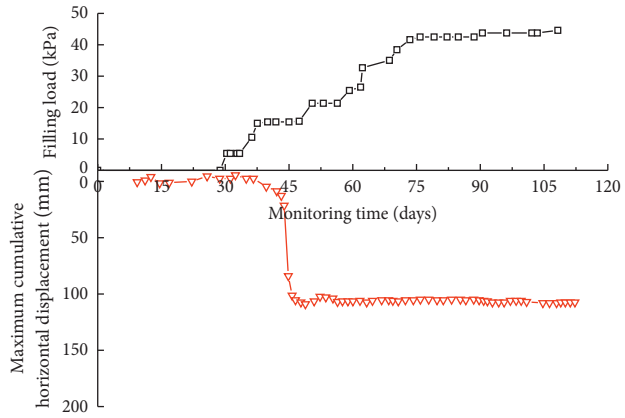

Figure 17: Variation of maximum cumulative horizontal displacement with filling load.

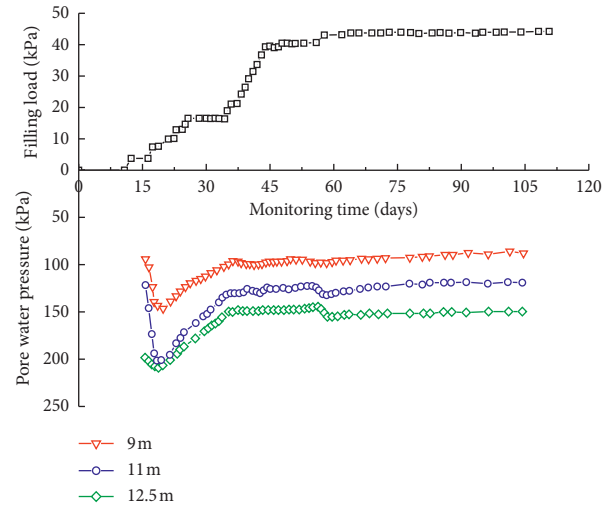

Figure 18: Variation of pore water pressure with filling load.

filling rate, and the excess pore water pressure gradually stabilized when the embankment construction was completed. Therefore, during embankment construction, controlling the construction rate of the pipe piles and embankment in a reasonable range is necessary to avoid producing excessive excess pore water pressure in a short period of time.

Figure 19 shows the variation curves of cumulative settlement with filling load in section K64 + 080. The final settlements are within a reasonable range, and the main settlements of embankment occur in the embankment filling period because a fast embankment filling rate results in a rapid settlement rate. After the completion of embankment filling, the settlements began to converge and gradually tend to stabilize. Therefore, reasonable filling rate can decrease the settlement rate and maintain the stability of the embankment.

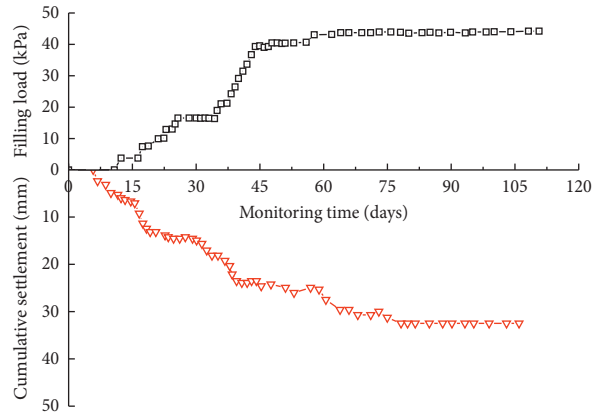

Figure 19: Variation of cumulative settlement with filling load.

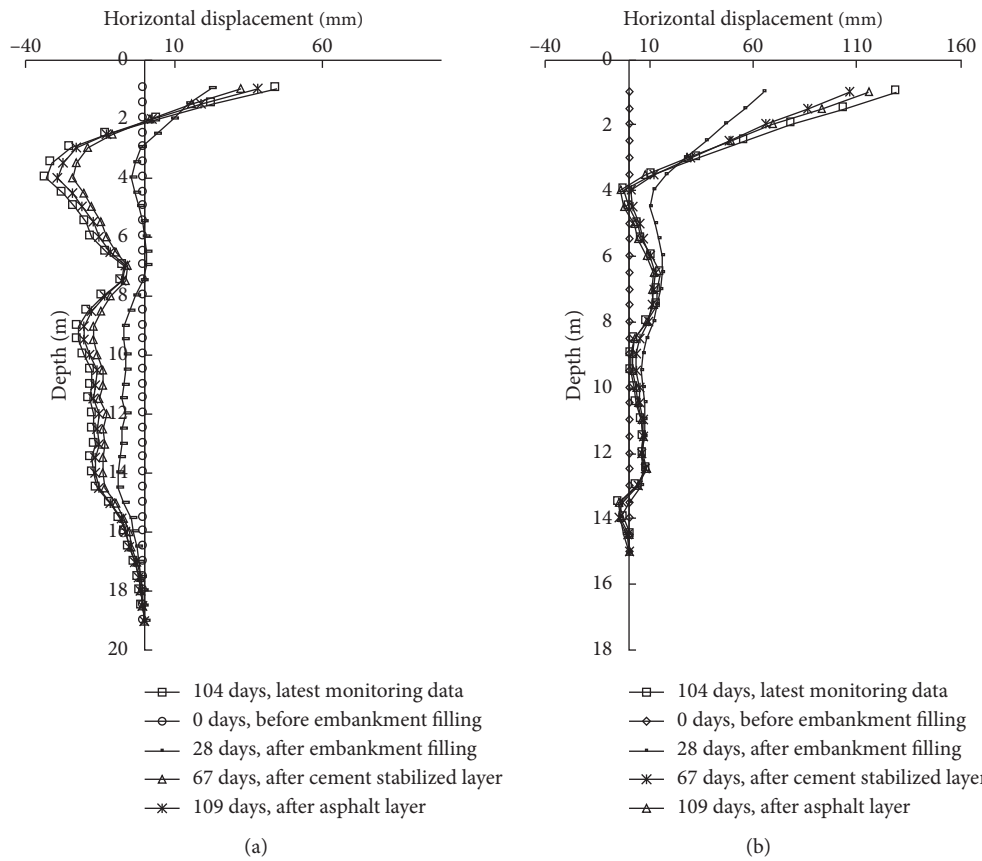

Figure 20: Variation of cumulative horizontal displacement in different construction stages. (a) Left embankment. (b) Right embankment.

Figure 20 shows the variation of cumulative horizontal displacement of section K64 + 080 in different construction stages, and Figure 21 shows the variation of cumulative displacement with filling load in the left section of K64 + 080. Figure 20 shows that horizontal displacement mainly occurred during embankment filling, and evident turning was observed at the foundation depth of 4 m, both sides of section K64 + 080, small horizontal displacements in the lower part, and large horizontal displacements in the upper part. The reason is that the overburden pressure has a certain offset influence on the soil squeezing effect. After embankment filling, the horizontal displacement increased because the reconstructed pipe piles are used to fix the collapsed embankment, and the horizontal displacement of soil is changed by the soil squeezing effect of the pipe piles. With embankment filling and surface construction, the shallow horizontal displacement increased, but the deep horizontal displacement bounced back because the influence of embankment load on the horizontal displacement is mainly concentrated in the shallow foundation. However, it has minimal influence on deep foundation, because the soil squeezing effect of the pipe pile gradually dissipates, and the

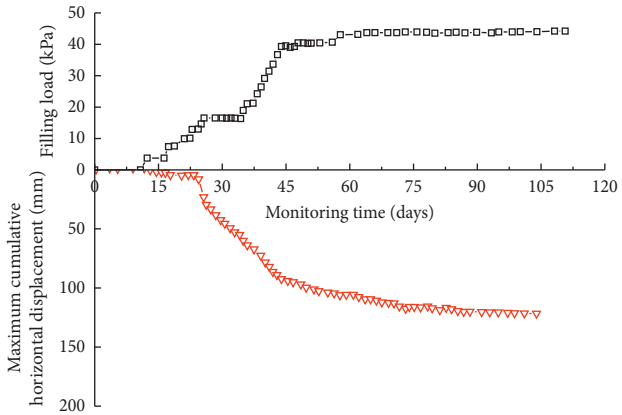

Figure 21: Variation of maximum cumulative horizontal displacement with filling load.

deep horizontal displacement has a certain degree of rebound. From the point of value, all horizontal displacement values are within the allowable limits of the standards. After the construction of cement-stabilized layer was completed, the horizontal displacement has stabilized. In Figure 21, although the change rate of the maximum cumulative horizontal displacement is fast, it had shown convergence tendency after the completion of embankment filling. Therefore, the reconstructed pipe pile has a significant effect on limiting the horizontal displacement of the foundation.

5. Conclusion

The causes of sliding and cracking of embankment on the rigid column-improved soft soil were observed, the remediation measures were presented, and the reinforcement effect of the failed embankment was analyzed in this paper based on the actual problems in the construction of Xintai Expressway South Extension Project. The following conclusions can be drawn:

(1) The design pile spacing is too large, and the design bearing capacity of single pile is low due to the large safety factor of the embankment stability on rigid column-improved soft soil calculated by the existing code method, resulting in more loading shared by subsoil between piles, large settlement and displacement of foundation, and bending and fracture of some rigid column.

(2) The revised density method can be used to check the stability of flow sliding instead of the methods specified in the present codes. In addition, the bending moment of piles should also be checked to avoid the actual maximum bending moment from being larger than the design value.

(3) The perpendicularity deviation and joint quality of pipe piles, which may decrease the bearing capacity of single pile and lead to the bending failure of piles, should be emphasized.

(4) Excessive fill thickness that blows the pile caps causes the excessive load imposed on the soft subsoil between piles, thereby resulting in the excessive settlement of the foundation. Therefore, the elevation of pile caps and the fill thickness below the pile caps should be controlled in a reasonable range at the construction stage. If necessary, light embankment fillers (e.g., fly ash and foam polystyrene (EPS)) can be used to reduce the additional stress in the foundation.

(5) The reconstruction of additional piles in the sliding section and APDHs in the cracking section can reduce the postconstruction settlements and horizontal displacements effectively. Such findings have been validated by the measured excess pore water pressure, subgrade settlement, and horizontal displacement. However, the soil squeezing effect accompanied along with the pile construction has adverse impact on embankment stability. Thus, a reasonable construction rate of piles should be selected to diminish this impact.

Data Availability

The data used to support the findings of this study are available from the corresponding author upon request.

Conflicts of Interest

The authors declare that there are no conflicts of interest regarding the publication of this paper.

Acknowledgments

This study was supported by the National Natural Science Foundation of China (51208517; 51778634) and Hunan Provincial Natural Science Foundation of China (2019JJ40344). The authors are grateful to Professor Jifu Liu at Guangdong Province Communication Planning and Design Institute Co., Ltd., for his help in providing the systemic project information and data.

References

[1] W. Liu, S. Qu, H. Zhang, and Z. Nie, "An integrated method for analyzing load transfer in geosynthetic-reinforced and pile-supported embankment," *KSCE Journal of Civil Engineering*, vol. 21, no. 3, pp. 687–702, 2017.

[2] G. M. Filz, J. A. Sloan, P. Michael, M. P. McGuire, M. Smith, and J. Collin, "Settlement and vertical load transfer in column-supported embankments," *Journal of Geotechnical and Geoenvironmental Engineering*, vol. 145, no. 10, Article ID 04019083, 2019.

[3] W. H. Lu, L. C. Miao, F. Wang, J. H. Zhang, Y. X. Zhang, and H. B. Haibo Wang, "A case study on geogrid-reinforced and pile-supported widened highway embankment," *Geosynthetics International*, vol. 27, no. 3, pp. 261–274, 2019.

[4] X. H. Zhu and G. M. Shu, "Causes analysis of embankment slide near Xinwei viaduct of Guangzhou-Zhuhai north expressway," *Journal of China & Foreign Highway*, vol. 26, no. 4, pp. 27–29, 2006.

[5] A. Q. Li, "Failure analysis on CFG pile used for reinforcement of soft soil embankment," *Railway Standard Design*, no. 6, pp. 36–39, 2012.
[6] J. F. Liu, G. Zheng, and G. F. An, "Stability analysis of flow-slide of embankment on rigid-piles composite ground," *Geotechnical Investigation & Surveying*, vol. 35, no. 6, pp. 17–22, 2013.
[7] J. Y. Mo and X. P. Huang, "Analysis of foundation failure of mineral yard," *Port and Waterway Engineering*, vol. 10, pp. 212–217, 2013.
[8] R. L. Michalowski, A. Wojtasik, A. Duda, A. Florkiewicz, and D. Park, "Failure and remedy of column-supported embankment: case study," *Journal of Geotechnical and Geoenvironmental Engineering*, vol. 144, no. 3, p. 10, 2018.
[9] J. C. Chai, S. Shrestha, and T. Hino, "Failure of an embankment on soil-cement column– improved clay deposit: investigation and analysis," *Journal of Geotechnical and Geoenvironmental Engineering*, vol. 145, no. 9, Article ID 05019006, 2019.
[10] JTG/Td31-02-2013, "Industrial Recommendation Standard of the People's Republic of China, JTG/Td31-02-2013," *Technical Guidelines for Design and Construction of Highway Embankment on Soft Ground*, People's Communications Press, Beijing, China, 2013.
[11] JTG D30-2015, "Industry Standard of the People's Republic of China, JTG D30-2015," *Specifications for Design of Highway Subgrades*, People's Communications Press, Beijing, China, 2015.
[12] G. Zheng, L. Liu, and J. Han, "Stability of embankment on soft subgrade reinforced by rigid piles (II): group piles analysis," *Chinese Journal of Geotechnical Engineering*, vol. 32, no. 12, pp. 1811–1820, 2010.
[13] G. Zheng, X. Yang, H. Zhou, and J. Chai, "Numerical modeling of progressive failure of rigid piles under embankment load," *Canadian Geotechnical Journal*, vol. 56, no. 1, pp. 23–34, 2019.
[14] M. Kitazume, K. Orano, and S. Miyajima, "Centrifuge model tests on failure envelope of column type deep mixing method improved ground," *Soils and Foundations*, vol. 40, no. 4, pp. 43–55, 2000.
[15] British Standard 8006-1, *Code of Practice for Strengthened/reinforced Soils and Other Fills*, British Standards Institution, London, UK, 2010.
[16] J. F. Liu, S. Y. Guo, and C. J. Xiao, "Revised density method for stability analysis of flow slide of embankment with concrete-pile composite foundation," *Guangdong Highway Communications*, vol. 146, no. 5, pp. 12–20, 2016.
[17] J. F. Liu and G. Zheng, "Influences of bearing capacity of piles on stability of embankment with rigid pile composite foundation," *Chinese Journal of Geotechnical Engineering*, vol. 41, no. 11, pp. 1992–1999, 2019.
[18] A. Wang, D. Zhang, and Y. Deng, "Lateral response of single piles in cement-improved soil: numerical and theoretical investigation," *Computers and Geotechnics*, vol. 102, pp. 164–178, 2018.
[19] CRCC Harbour and Channel Engineering Bureau Group Survey & Design Institute Co., Ltd., *Cause Analysis of Subgrade Collapse of k64+080~k64+180 South Extension of Xintai Expressway*, CRCC Harbour and Channel Engineering Bureau Group Survey & Design Institute Co., Ltd., Guangzhou, China, 2015.
[20] R. P. Chen, Y. M. Chen, J. Han, and Z. Z. Xu, "A theoretical solution for pile-supported embankments on soft soils under one-dimensional compression," *Canadian Geotechnical Journal*, vol. 45, no. 5, pp. 611–623, 2008.
[21] D. S. Miao, J. F. Liu, and Z. B. Shi, "Application of appear shear strength method on analysis of pile concrete failure of composite foundation for embankment," *Guangdong Highway Communications*, vol. 141, no. 6, pp. 34–43, 2015.
[22] CRCC Harbour and Channel Engineering Bureau Group Survey & Design Institute Co., Ltd., "Summary report on the third party monitoring of soft soil foundation of south extension project of Xintai Expressway in Guangdong Province," CRCC Harbour and Channel Engineering Bureau Group Survey & Design Institute Co., Ltd., Guangzhou, China, 2016.